PmaI-dependent pH gradients initiate inter- and intraspecies germling fusion in filamentous fungi

Rudolph A. Y.[1], Rotermund, N.[2], Vasilevska, N.[1], Fleißner A.[2], Nordzieke D.E.[1,*]

[1]University of Göttingen, GZMB, Institute of Microbiology and Genetics, Genetics of Eukaryotic Microorganisms, Grisebachstr. 8, 37077 Göttingen, Germany

[2]University of Braunschweig, Institute of Technology, Institute of Genetics, Spielmannstraße 7, 38106 Braunschweig, Germany

*Correspondence: dnordzi@gwdg.de

Keywords: *Colletotrichum graminicola*, *Neurospora crassa*, *Botrytis cinerea*, PmaI ATPase, fungal GPCR, MAPK pathway, CAT fusion

Abstract

Somatic cell fusion among spore germlings is a complex process in filamentous fungi that enables the formation of a syncytial unit and facilitates the exchange of genetic material apart from sexual reproduction. In this study, we investigated the molecular mechanisms underlying germling fusion in the maize pathogen *Colletotrichum graminicola*. Based on secretomes harvested during the germling fusion process of fusion-competent oval and fusion-deficient falcate conidia, we identified pH as a communication signal. We showed that the plasma membrane localized ATPase PmaI is a probable source for pH gradient formation. Our results also suggest that the a-pheromone receptor CgSte3 mediates sensing of acidic pH gradients, activating downstream the Cell Wall Integrity Mitogen Activated Protein Kinase pathway. We propose a new model for germling interactions, in which pH serves as an interaction initiation signal, resulting in the activation of the cell-dialogue. Our findings have implications for our understanding of fungal communication and pathogenicity, and highlight the importance of pH as a signal molecule in germling fusion.

Introduction

Somatic cell fusion is a complex process that enables filamentous fungi to merge genetically identical or non-identical cells, resulting in the formation of a syncytial unit. This process is essential for the efficient development and growth of fungal colonies, and is mediated by a variety of signaling pathways and molecular mechanisms (Bastiaans *et al.*, 2015, Richard *et al.*, 2012, Herzog *et al.*, 2015). In *Neurospora crassa*, a model organism for studying fungal biology, somatic cell fusion is initiated by the germination of conidia, which undergo mutual attraction and fusion to form a syncytial unit (Read *et al.*, 2012). This process is regulated by a complex interplay of signaling molecules and molecular components, including transcription factors, the striatin-interacting phosphatase and kinase (STRIPAK) complex, NADPH oxidase complexes, and mitogen-activated protein kinase (MAPK) pathways (Fischer and Glass, 2019).

The current understanding of germling fusion in fungi suggests that it is a three-step process: (I) the formation of conidial anastomosis tubes (CATs), (II) bidirectional chemotropic growth of

CATs towards each other (CAT homing), and (III) cell fusion at the CAT contact side (Glass *et al.*, 2004, Kurian *et al.*, 2018). Central to the reciprocal recognition of interaction partners are the two proteins SO (soft) and MAK-2, which are part of the cell wall integrity (CWI) and pheromone Mitogen Activated Protein Kinase (MAPK) pathways, respectively (Fleissner *et al.*, 2009, Serrano *et al.*, 2018). During the tropic growth of the interacting cells, both proteins are recruited to the plasma membrane of the growing cell tips in an alternating manner. The current hypothesis proposes that SO localization to the CAT tip is associated with the release of a previously unknown communication signal, which is recognized by MAK-2 in the interaction partner, forming the so-called 'cell-dialogue' (Fleissner et al., 2009). Recent studies have challenged the long-held assumption that germling fusion occurs only among germlings of the same species, revealing that interspecies interactions and true fusion can occur between different fungal species (Haj Hammadeh *et al.*, 2022, Mehta and Baghela, 2021). For example, germlings of *N. crassa* and *Botrytis cinerea* interact with each other albeit the fusion process is not completed (Haj Hammadeh et al., 2022). Additionally, *Colletotrichum gloeosporioides* and *Colletotrichum siamense* fuse and form viable progeny, with the genome of the resulting progeny undergoing genetic recombination (Mehta and Baghela, 2021).

Colletotrichum graminicola is a hemibiotrophic maize pathogen responsible for anthracnose disease, causing high economic damage with corn loss of 10-20% of harvest annually (Belisário *et al.*, 2022). For successful disease development, *C. graminicola* generates two different asexual spore types, falcate conidia in acervuli on infected maize leaves, and oval conidia inside parenchyma cells nearby the plant vascular system (Belisário et al., 2022, Panaccione *et al.*, 1989). Those spore types differ significantly in their vegetative development and infection-relevant processes, making falcate conidia more efficient in leaf infection and enable oval conidia to sense maize root-exudated signals, followed by chemotropic growth towards the host and root infection (Nordzieke *et al.*, 2019, Schunke *et al.*, 2020, Rudolph *et al.*, 2024a, Chaky *et al.*, 2001). One prominent difference between both spore types is the ability to form a network by vegetative fusions: oval conidia form fusion bridges at high rates under starvation conditions, whereas falcate conidia stay dormant in the same experimental setups. However, close proximity of oval and falcate conidia can release dormancy in falcate conidia and result in fusion of both spore types (Nordzieke et al., 2019). From these results we conclude that the germling interaction signal is secreted by oval conidia but is absent from falcate conidia. Intriguingly, oval conidia fusion takes place also on leaves. There, fusion bridge formation is correlated to the generation of hyphopodia for leaf penetration, although both processes do not directly depend on each other (Nordzieke et al., 2019, Nordzieke, 2022).

In this study, we aimed to identify signals responsible for reciprocal germling attraction during the fusion process in *C. graminicola*. To identify these signal(s), a methodical setup was established and verified, enabling us to collect secreted molecules during the fusion process. Comparing the germling fusion secretome of oval and falcate conidia, we observed difference in secretome pH. In the following, we verified that distinct pHs are able to attract *C. graminicola* germlings and medium pH influences CAT fusion frequency. We further explored that the a-pheromone receptor CgSte3 and the CWI pathway mediate pH sensing. Applying an inhibitor of the plasma membrane standing ATPase PmaI, we provided evidence that pH signal formation is dependent on ATPase activity and links germination and fusion in *C. graminicola*. From those findings, we propose a new model for germling interactions, in which pH serves as an interaction initiation signal, resulting in the activation of the cell-dialogue. Since PmaI-dependent pH gradients are formed in all fungi in the course of germination, we further explored intraspecies interaction of *C. graminicola* with *N. crassa* and *B. cinerea*. All together, we identified that pH gradients serve as signal during reciprocal germling attraction prior to fusion in *C. graminicola*. Since the fusion rate of other filamentous fungi does depend on pH as well, we propose a general function as interaction initiation signal.

Material and methods

Strains, growth conditions, and collection of spores

The *C. graminicola* (Ces.) G.W. Wilson (teleomorph *Glomerella graminicola* D. J. Politis) wild-type strain M2 (also referred to as M1.001) was provided by H. Deising (Martin-Luther University Halle-Wittenberg) and used in this study (Forgey *et al.*, 1978, O'Connell *et al.*, 2012). Falcate and oval conidia of *C. graminicola* were generated and collected as described previously (Rudolph *et al.*, 2024b). *N. crassa* matA (strain FGSC2489 provided by Fungal Genetics Stock Center) and *B. cinerea* (strain B05.10; Quidde *et al.*, 1999) were grown on Vogel´s minimal medium (Vogel´s MM), supplemented with 2% sucrose (Vogel, 1956). All strains used in this study are listed in Supplementary Table 1.

Generation and analysis of germling secretome during conidial interaction

In our standard protocol for the quantification of germling fusions, we spread 50 µl of spore solution (c = 5 x 10^7 ml^{-1}) on water agar (1% serva agar, 1% agarose, 25 mM $NaNO_3$) and incubate the plates for 17 h at 23°C. For oval conidia preparations, we see a high percentage of germling interacting and fusing after that time. However, falcate conidia do not germinate nor fuse under these conditions (Nordzieke et al., 2019). To enable the identification of signals generated during the germling interaction and fusion process, we aimed to collect the secretome of oval and falcate in this experimental setup and to compare their chemical properties. Therefore, we spread oval and falcate conidia of *C. graminicola* CgM2 on cellophane (SERVA cellophane sheets II (140 x 133), SERVA Electrophoresis GmBH, Heidelberg, Germany; 50 µl of spore solution with c = 5 x 10^7 ml^{-1}) topping water agar and let the liquid evaporate (clean bench). Afterwards, the cellophane sheets were transferred to petri dishes filled with a single layer of glass beads (Glass Beads Ø 2.85 – 3.45 mm, Roth, Karlsruhe, Germany) and 10 ml of a 25 mM $NaNO_3$ solution. After 17 h incubation at 23°C, the liquid was collected in glass ware and frozen at -80°C. To control the formation of germling fusion networks, microscopic pictures were taken, verifying the formation of fusion bridges for oval conidia and their absence for falcate conidia (Figure 1). pH of secretome solutions was measured using pH strips (20RO5121, Roth, Karlsruhe, Germany) of freshly harvested or 10 x concentrated secretome.

Germling fusion and germination assays in *C. graminicola*

To determine the impact of concentrated germling fusion secretome on the fusion and germination ability of oval and falcate conidia, 10 µl of different concentrated spores solutions (c = 10^6 ml^{-1}; 5 x 10^5 ml^{-1}; 10^5 ml^{-1}) were dropped on water agar (1% serva agar, 1% agarose, 25 mM $NaNO_3$) and dried under a laminar flow. The dried spore drops were topped with 20 µl of 10 x concentrated secretome generated from oval or falcate conidia germlings during fusion conditions. After drying of the secretome drops, the plates were inoculated for 17 h at 23°C. At least 100 touching germlings and conidia were accessed for fusion bridge formation and 100 conidia for germination in at least three biological replicates.

For the determination of pH-dependent germling fusion and germination frequencies, 50 µl of oval conidia (c = 5 x 10^7 ml^{-1}) were spread on water agar (1% serva agar, 1% agarose, 25 mM $NaNO_3$) adjusted to different pH values after autoclaving using pH strips (pH-Fix 4.5-10.0, Roth, Karlsruhe, Germany). For buffered conditions, the water agar was prepared with citrate phosphate buffer to reach a stable pH of 6.5. Microscopic evaluation was performed after 17 h of cultivation at 23°C, counting at least 100 touching conidia or germlings and accessing

140 their fusion state. Germination rates were determined by evaluating at least 100 conidia. Both
141 experiments were performed in at least three biological replicates.

142 Concentration-dependent germling fusion assays were performed by dropping 10 µl of oval
143 conidia spore solution (10^6 m^{-1}; 7.5 x 10^5 m^{-1}; 5 x 10^5 m^{-1}; 2.5 x 10^5 m^{-1}; 10^5 m^{-1}; 7.5 x 10^4 m^{-1};
144 5 x 10^4 m^{-1}) of *C. graminicola* wildtype (CgM2), *Cgste3* deletion and complementation strains
145 on water agar (1% serva agar, 1% agarose, 25 mM $NaNO_3$), dried under laminar flow, and
146 incubated for 17 h at 23°C. For higher concentrations, at least 100 touching conidia or
147 germlings were microscopically analyzed for the presence of fusions, for lower concentrations
148 the maximal amount of conidia and germlings present in the 10 µl drop were evaluated. For
149 each concentration, the experiments were performed at least three times.

150 To determine the effect of PmaI inhibitor Demethoxycurcumin (DMCM; Demethoxycurcumin ≥
151 98% HPLC, Sigma-Aldrich, St. Louis, USA) on germling fusion and germination rate of oval
152 conidia, DMCM was dissolved in DMSO. Working solutions were prepared just before use by
153 further diluting with distilled water. As control, diluted DMSO concentration was used
154 equalizing 15 µM of DMCM. 20 µl of different DMCM concentrations or the control were applied
155 on dried 10 µl drops of oval conidia (c = 10^6 ml^{-1}) on water agar (1% serva agar, 1% agarose,
156 25 mM $NaNO_3$) and dried as well under a laminar flow. Microscopic evaluation was performed
157 after 17 h of cultivation at 23°C, counting at least 100 touching conidia or germlings and
158 accessing their fusion state. Germination rates were determined by evaluating at least 100
159 conidia. Both experiments were performed in at least three biological replicates.

160

161 Chemotropic assay

162 Chemotropic growth is defined as directed growth along a gradient of a given chemical
163 stimulus, which can be positive (attractant signal) or negative (repellant signal). To display
164 positive and negative chemotropic growth responses, the 'chemotropic index' is used as a
165 standard for result depiction, indicating the difference of a preferred growth direction compared
166 to a situation, in which neither attraction no repulsion occurs (Turrà *et al.*, 2015). In our lab, we
167 developed a 3D printed device to easily monitor directed growth responses (Schunke et al.,
168 2020). Using this device, we determined growth direction of fungal germlings derived from *C.*
169 *graminicola* oval conidia of CgM2 (wildtype), Δ*Cgste3*, Δ*Cgso*, and the corresponding
170 complementation strains after incubation for 6 h at 23°C. As attractant molecules, we evaluated
171 10 x concentrated secretome of oval and falcate conidia generated during the germling fusion
172 process and potassium phosphate buffer adjusted to different pH values (pH 6, 7, ,7.5, 8). All
173 experiments were performed in at least two biological replicates.

174

175 Microscopy

176 Light (differential interference contrast (DIC)) was performed with the AxioImager M1
177 microscope (Zeiss, Jena, Germany). Images were captured with the Photometrix coolSNAP
178 HQ camera (Roper Scienific, Photometrics, Tucson, AZ, USA) and processed with the ZEISS
179 ZEN software (version 2.3, Zeiss). Alternatively, images were taken with the Axio Observer
180 microscope (Zeiss, Jena, Germany). Images were captured with sCMOS pco.panda 4.2 M
181 (Excelitas PCO GmbH) and processed with the software 4-D MICROSCOPE FLMV 1.1 and 4-
182 D MICROSCOPE Observer Z.1 (Schnabel et al., 1997).

183

184

185 Inter- and intraspecies interaction studies

186 The interspecies interaction experiments were performed on Vogel´s MM (20 ml of 50x Vogel's
187 trace elements solution, 20 g Sucrose, 15 g Agar-Agar; Vogel, 1956). The interactions
188 experiment with *C. graminicola* and *B. cinerea* was carried out at 23°C with an incubation time
189 of 17 h. First, fungal spore solutions were adjusted to distinct concentrations (*B. cinerea*: c =
190 3.33 x 10^7 ml^{-1}; *C. graminicola*: c = 5 x 10^7 ml^{-1}). 300 µl of *B. cinerea* spore solutions were
191 plated on Vogel's MM medium and 50 µl of *C. graminicola* oval conidia added. Using a pipette
192 tip, the spores from both species were mixed and spread onto the medium plate. For the
193 interspecies interaction experiment between *C. graminicola* and *N. crassa*, 50 µl of a
194 *C. graminicola* oval conidia spore solution (c = 5x10^7 x ml^{-1}) was first distributed on Vogel´s
195 MM medium using glass beads and incubated for 14 h at room temperature. After that time,
196 300µl of *N. crassa* spore solution (c = 10^7 ml^{-1}) was added on those pre-incubated plates, dried
197 and further incubated at 28°C for 3.5 - 4 h. The interspecies interaction rate was calculated
198 based on several screen fields in which spores of both species were present. In total, ≥ 76
199 interactions were calculated in three biological replicates.

200 pH-dependent fusion and germination rates of *C. graminicola*, *B. cinerea*, and *N. crassa* was
201 performed on Vogels' MM adjusted to distinct pH without buffering the medium. For
202 *C. graminicola*, 50 µl of oval conidia spore solution (c = 5x10^7 x ml^{-1}) was spread on Vogels'
203 MM using glass beads. For *B. cinerea* and *N. crassa*, 300 µl of c = 10^7 ml^{-1} spore solutions of
204 were added on Vogels' MM and spread using pipette tips. After incubation (*C. graminicola*: 17
205 h, 23°C, *B. cinerea*: 17 h, 23°C, *N. crassa*: 3 h, 30°C), at least 100 contacting germlings or
206 conidia were accessed for formed fusion bridges. In the same experiments, germination rates
207 were determined from at least 100 conidia. Both fusion and germination experiments were
208 conducted in at least 3 biological replicates.

209 Localization of MAK-2-GFP was monitored during *N. crassa* – *N. crassa* and *N. crassa* –
210 *C. graminicola* interactions, using the same conditions described above. As readout served
211 fluorescence microscopy.

212

213 Statistics

214 For statistical analysis in this study, the T-test for unequal variances was used for all
215 experiments (Ruxton, 2006).

216

217 AI statement

218 The AI chatbot 'Chat AI' provided by the GWDG at the Georg-August University Göttingen was
219 used to improve the text of this manuscript regarding English grammar and typing.

220

221 <u>Results</u>

222 Molecules secreted from oval conidia during fusion induce chemotropic growth of *C.*
223 *graminicola* germlings

224 While numerous proteins and second messengers are necessary for CAT fusion (Fu *et al.*,
225 2011, Fischer and Glass, 2019), signals resulting in bidirectional attraction of germlings are
226 unknown. To explore the potential of CAT signal identification, we established an experimental
227 design enabling to harvest secreted signals during fusion bridge formation. We spread equal
228 amounts of fusion competent oval or fusion-incompetent falcate conidia on cellophane sheets

229 topping water agar. After drying the spore solution, we transferred the cellophane to a new
230 petri dish filled with a single layer of glass beads and 25 mM $NaNO_3$ solution. After 17 h of
231 incubation, the germination and fusion state of the cultures were evaluated, showing that oval
232 conidia germinated in high percentages and undergo fusions eagerly. In contrast, falcate
233 conidia did not germinate or form fusion bridges (Figure 1, A). Since those results are in line
234 with previous observations (Nordzieke et al., 2019), glass beads and liquid were separated by
235 filtration and the flow through analyzed.

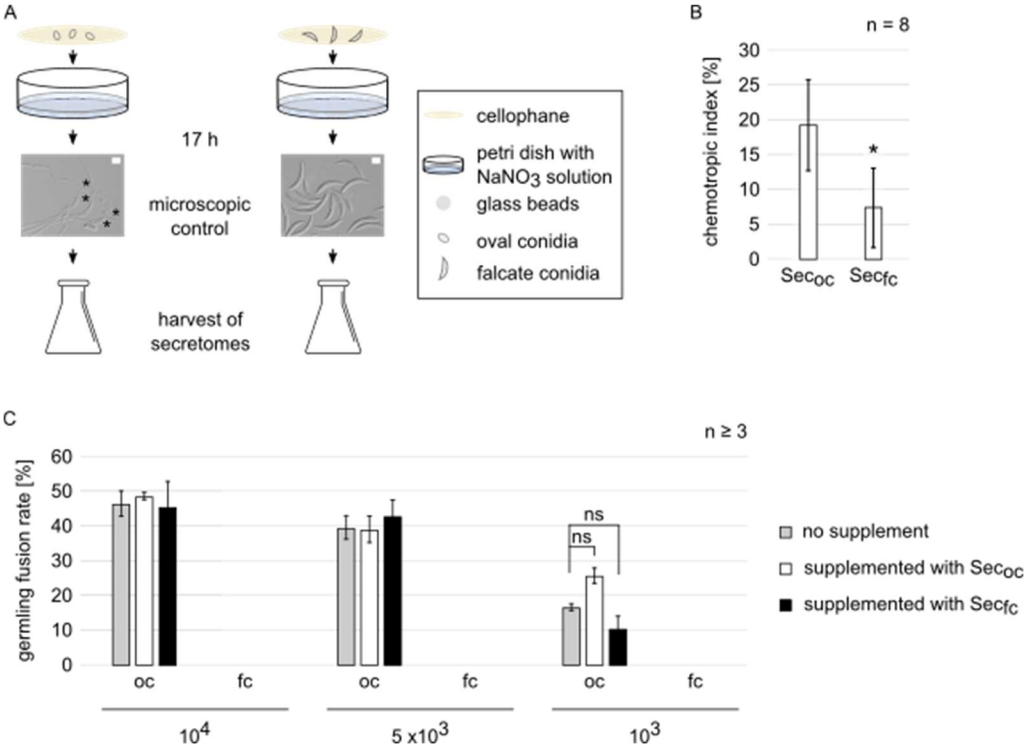

236

237 **Figure 1** CAT secretome of *C. graminicola* oval conidia elicits chemotropic growth and shapes fusion
238 and germination of oval and falcate conidia. (A) Schematic representation of fusion secretome
239 generation. 50 µl of oval and falcate conidia spore solutions (c = 5 x 10^7 ml^{-1}) of the *C. graminicola*
240 wildtype were spread on cellophane topping water agar. After evaporation of the liquid, cellophane
241 sheets were transferred to petri dishes filled with a single layer of glass beads and 10 ml of a 25 mM
242 $NaNO_3$ solution. After 17 h incubation at 23°C, the fusion secretome was collected and the cellophane
243 evaluated for the presence or absence of fusions. (B) Chemotropic index of *C. graminicola* germlings
244 derived from oval conidia to 10 x concentrated fusion secretome harvested from oval (Sec_{oc}) or falcate
245 (Sec_{fc}) conidia incubations. 20 µl of oval conidia (c = 5 x 10^5 ml^{-1}) were applied in a 3D printed device
246 between two wells containing 40 µl solvent control and attractant. Microscopic evaluation of fungal tip
247 growth was performed after incubation for 6 h, 23°C, n = 8 biological replicates, statistical significance
248 was calculated with a two-tailed t-test (*, $p < 0.05$). (C) Germling fusion rates in dependence of spore
249 concentration and the supplementation with 10 x concentrated Sec_{oc} and Sec_{fc}. 10 µl of oval or falcate
250 conidia were dropped in different amounts (10^4, 5 x 10^3, 10^3) on water agar plates agar (1% serva agar,
251 1% agarose, 25 mM $NaNO_3$). After drying, the drops were topped with 20 µl of 10 x concentrated Sec_{oc}
252 and Sec_{fc} and the liquid dried again. After 17 h incubation at 23°C, at least 100 contacting germlings
253 and conidia were microscopically examined for the formation of fusion bridges, n ≥ 3, ns = not significant.

254

255 In a first experiment, we tested whether the fusion secretomes of oval and falcate conidia are
256 able to attract *C. graminicola* germlings using a 3D printed device developed in our group
257 (Schunke et al., 2020). Indeed, we found that 10x concentrated fusion secretome from oval
258 conidia (Sec_{oc}) induce a strong chemotropic response, whereas the 10x concentrated fusion

259 secretome of falcate conidia (Sec_{fc}) showed minor attraction potential (Figure 1, B), indicating
260 a successful harvest of interaction signal(s). In a second approach, we supplemented oval and
261 falcate conidia with 10x Sec_{oc} and Sec_{fc} and accessed their germination and fusion rates after
262 17 h of incubation. Since germling fusion is a spore concentration-dependent process, we
263 tested the effect of the secretomes on optimal (10^4) and suboptimal (10^3) spore concentrations
264 (Figure 1, C, Supplementary Figure S1). For oval conidia, we observed a spore-density
265 dependent effect of the secretomes: whereas in optimal experimental conditions, no effect of
266 secretome addition was visible, 10x Sec_{oc} did increase the fusion frequency of oval conidia
267 applied in suboptimal concentrations (Figure 1, C). Regarding falcate conidia, the addition of
268 concentrated Sec_{oc} or Sec_{fc} did not induce fusions; however, in experimental conditions with
269 10^3 applied spores, germination of this spore type was induced (Supplementary Figure S1).
270 Together, these first experiments indicate that isolation of a CAT fusion signal was successful
271 with the experimental approach chosen and point to a possible interconnection between
272 germination and fusion.

273

274 Distinct pHs attract *C. graminicola* germlings and induce germling fusion

275 Next, we aimed on secretome characterization. When we monitored the pH of the Sec_{oc} and
276 Sec_{fc} and compared it with control conditions, we observed a more basic pH for 10x Sec_{oc}
277 (Figure 2, A). We thus aimed to explore, whether pH can act as attractant for *C. graminicola*
278 and influence fusion frequency. As depicted in Figure 2, B, pH of 7.5 strongly attracts
279 germlings, whereas higher or lower pH values do not, indicating the sensing is specific to
280 distinct pH gradients. Monitoring of CAT fusion events on water agar plates with adjusted pH
281 values revealed that in comparison to not adapted conditions, pH values of 5 and >7 are
282 inhibiting fusion bridge formation. In contrast, medium adjusted to pH 6.5 induces fusion
283 frequency. From these results, we were wondering whether pH could be a mere factor of
284 wellbeing for *C. graminicola* germlings, therefore enabling increased number of fusion events.
285 To test this, we generated buffered water agar medium with a pH adjusted to 6.5, which
286 provides optimal fusion condition in not buffered conditions. Intriguingly, no fusions were
287 detected in those experiments, underpinning the necessity of active pH change by fungal
288 germlings or conidia for fusion bridge formation (Figure 2, C). In the same experiments, we
289 also monitored germination. In contrast to network formation by fusion, the germination
290 process is only affected under buffered conditions (Supplementary Figure 2).

291

292 The a-pheromone receptor CgSte3 and the MAPK scaffold CgSo mediate pH sensing

293 In recent work of our group and others, fungal pheromone receptors were shown to perceive
294 defense molecules secreted from plant roots like peroxidases and diterpenoids besides fungal
295 pheromones (Rudolph et al., 2024a, Rudolph et al., 2024b, Turrà et al., 2015, Sridhar *et al.*,
296 2020, Sharma *et al.*, 2022, Ramaswe *et al.*, 2024, Vitale *et al.*, 2019). Similarly, the Cell Wall
297 Integrity Mitogen Activated Protein Kinase pathway (CWI) was shown to mediate the
298 extracellular signals and transform them into chemotropic growth responses (Turrà et al., 2015,
299 Sridhar et al., 2020, Sharma et al., 2022). To test whether this receptor-MAPK module is also
300 involved in pH sensing, deletion mutants of genes encoding for the a-pheromone receptor
301 *Cgste3* and the CWI scaffold *Cgso* were examined for their ability to sense and re-direct growth
302 to pH 7.5 (Figure 3). In contrast to wild-type strain CgM2, which show a strong growth re-
303 direction, both mutant strains fail to grow towards a gradient of pH 7.5. For both mutants, this
304 effect was restored by reintroducing the corresponding gene (Figure 3, A).

305

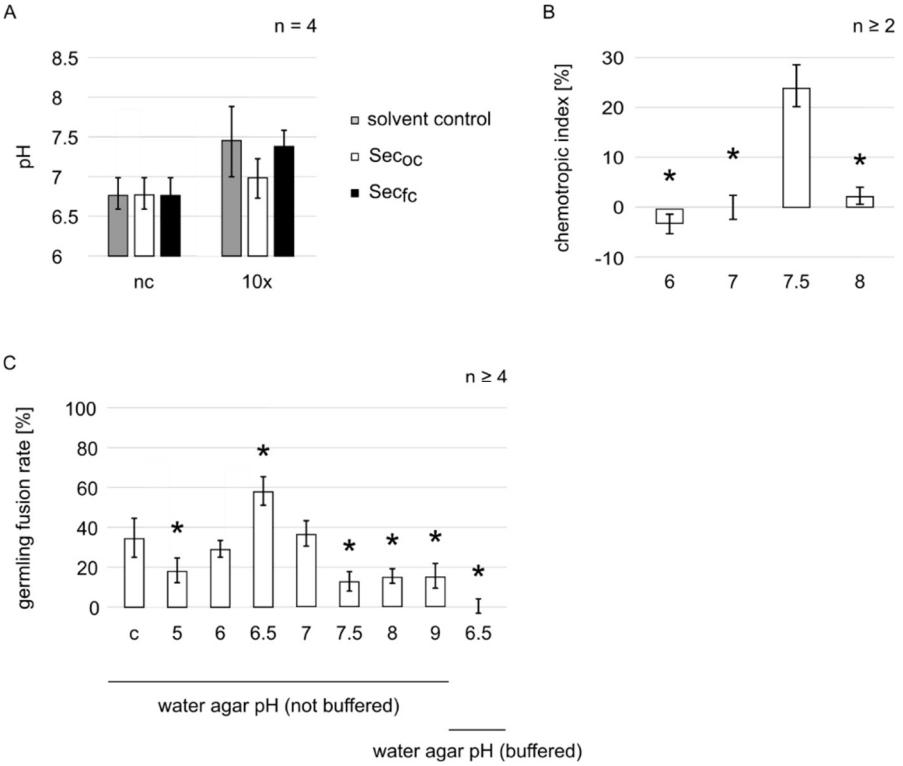

Figure 2 Distinct pH values attract *C. graminicola* germlings and impact their ability to undergo fusions. (A) pH of freshly harvested not-concentrated and concentrated fusion secretome of oval (Sec_{oc}) and falcate (Sec_{fc}) was examined using pH strips, n = 4. (B) Chemotropic index of *C. graminicola* wild-type germlings to potassium phosphate buffer adjusted to different pH values (pH 6; 7;7.5; 8). 20 µl of oval conidia (c = 5 x 10^5 ml^{-1}) were applied in a 3D printed device between two wells containing 40 µl solvent control and attractant. Microscopic evaluation of fungal tip growth was performed after incubation for 6 h, 23°C for least two biological replicates, statistical significance was calculated with a two-tailed t-test (*, $p < 0.05$). (C) Germling fusion rate of *C. graminicola* wild-type germlings spread on water agar (1% serva agar, 1% agarose, 25 mM $NaNO_3$) adjusted to different medium pH with and without buffering. 50 µl of oval conidia (c = 5 x 10^7 ml^{-1}) were spread on the corresponding medium plates. After 17 h of incubation at 23°C, at least 100 contacting germlings and conidia were microscopically examined for fusion bridge formation, n ≥ 4. Statistical significance was calculated with a two-tailed t-test corresponding to control conditions (c) *, $p < 0.05$.

In an earlier report, we investigated the impact of *Cgso* deletion on developmental processes in *C. graminicola*. Besides the absence of germling and hyphal fusion, this mutant shows a strong conidiation phenotype, provoked by the impaired nutrition of asexual fruiting bodies, the acervuli (Nordzieke, 2022). Therefore, Δ*Cgso* appear dark and generate increased levels of aerial mycelia compared to wildtype. In contrast, the a-pheromone receptor mutant Δ*Cgste3* shows normal level of conidiation, indicating that this strain is able to undergo vegetative fusions. Indeed, microscopic investigations showed normal fusion frequencies of Δ*Cgste3* compared to wildtype, when both strains are plated in optimal spore concentrations (Figure 3, B and C). Interestingly, a decrease in spore concentration revealed a significant reduction of Δ*Cgste3* fusion rate compared to wild-type CgM2, which was reversed in a *Cgste3* complementing strain. At the same time, Δ*Cgste3* germination rates don't differ from the wildtype (Figure S3). From these results, we concluded that pH might act as long-distance signaling molecule, able to guided conidia or germlings towards each other, but dispensable when germlings are in close proximitiy.

Next, we aimed to identify the source of pH gradient formation. In filamentous fungi and plants, growth is strictly correlated to the activity of a plasma membrane located ATPase, PmaI. This

337 ATPase pumps protons into the extracellular space, creating pH gradients used for the uptake
338 of diverse molecules (Portillo, 2000, Palmgren, 2001, Li *et al.*, 2022, Zhgun *et al.*, 2020). Since
339 *pmaI* is an essential gene in many organisms (Harris *et al.*, 1994), we decided to use a
340 Demethoxycurcumin (DMCM), a described inhibitor of PmaI (Dao *et al.*, 2016), to test a
341 probable impact of PmaI-dependent pH gradients for germling fusion. Intriguingly, we see a
342 concentration-dependent inhibition of germling fusion compared to control conditions (Figure
343 3 D). At the same time, germination is inhibited by DMCM, further indicating that germination
344 and fusion are interconnected processes.

345

346 Indications for pH as a conserved fungal fusion initiation signal

347 At first, germling fusion was considered as a highly species-specific process, providing only
348 germling interaction and fusion of individuals of the same species or communication group
349 (Heller *et al.*, 2016, Serrano et al., 2018). However, this perspective is changing. For
350 filamentous fungi like *N. crassa* and *B. cinerea*, intraspecies germling interaction and even the
351 induction of the SO-MAK-2-dependent cell dialog was shown (Haj Hammadeh et al., 2022).
352 However, those interactions never result in cross-species progeny. In *N. crassa – B. cinerea*
353 interactions, the fusion process is abolished upon contact of both interaction partners. Instead
354 of cell wall degradation to allow fusion, a cell wall thickens (Haj Hammadeh et al., 2022).
355 Additionally, there are reports about true fusions in between closely related species. The plant
356 pathogenic fungi *Colletotrichum gloeosporioides* and *Colletotrichum siamense* form progeny
357 after fusion, which show signs of genetic recombination of both parental species, making
358 intraspecies fusion a driver of evolution and host adaptation (Mehta and Baghela, 2021, Haj
359 Hammadeh et al., 2022). A prerequisite for intraspecies fusion is the presence of common or
360 very similar interaction signals, which could guide individuals of two different species towards
361 each other. Since PmaI-dependent pH gradients are formed by all fungi during conidial
362 germination, we were interested in testing, whether *C. graminicola* germlings are able to
363 interact with other fungal species.

364 In a first approach, we plated either fusion competent spores of *C. graminicola* and *B. cinerea*
365 or *C. graminicola* and *N. crassa* on Vogel's minimal medium, providing conditions for fusion
366 bridge formation in all three species. Since those fungi grow with different speed and have
367 distinct temperature optima, specific incubation times had to be chosen. For *C. graminicola –*
368 *B. cinerea* interactions, conidia were spread in different concentrations on Vogel's MM and
369 incubated at 23°C. Since *N. crassa* conidia germinate and fuse much faster than *C.*
370 *graminicola*, the latter was pre-incubated for 14 h. After that time-interval, *N. crassa* conidia
371 were added and both fungi incubated further at 28°C. Both described experimental setups
372 resulted in interspecies and intraspecies interactions, whereas the proportion of species-
373 species interactions was least (Figure 4, A - D).

374 The hallmark of germling interaction in *N. crassa* is the oscillatory cell-dialogue, in which SO
375 and MAK-2 show an alternate recruiting to the plasma membrane of interacting partners. At
376 the end of this dialogue, MAK-2 accumulates at the contact point. Intriguingly, in intraspecies
377 interactions with *N. crassa*, this late accumulation of MAK-2 was shown, indicating an intact
378 cell dialogue (Fleissner et al., 2009, Haj Hammadeh et al., 2022). To test whether this is true
379 for *N. crassa – C. graminicola* interactions as well, a *N. crassa* wildtype strain expressing MAK-
380 2-GFP was used in interaction studies with *C. graminicola*. Likewise as described for *N. crassa*
381 *– N. crassa* and *N. crassa – B. cinerea* interactions, MAK-2-GFP accumulates at the contact
382 point with *C. graminicola* germlings (Supplementary Figure 4).

383

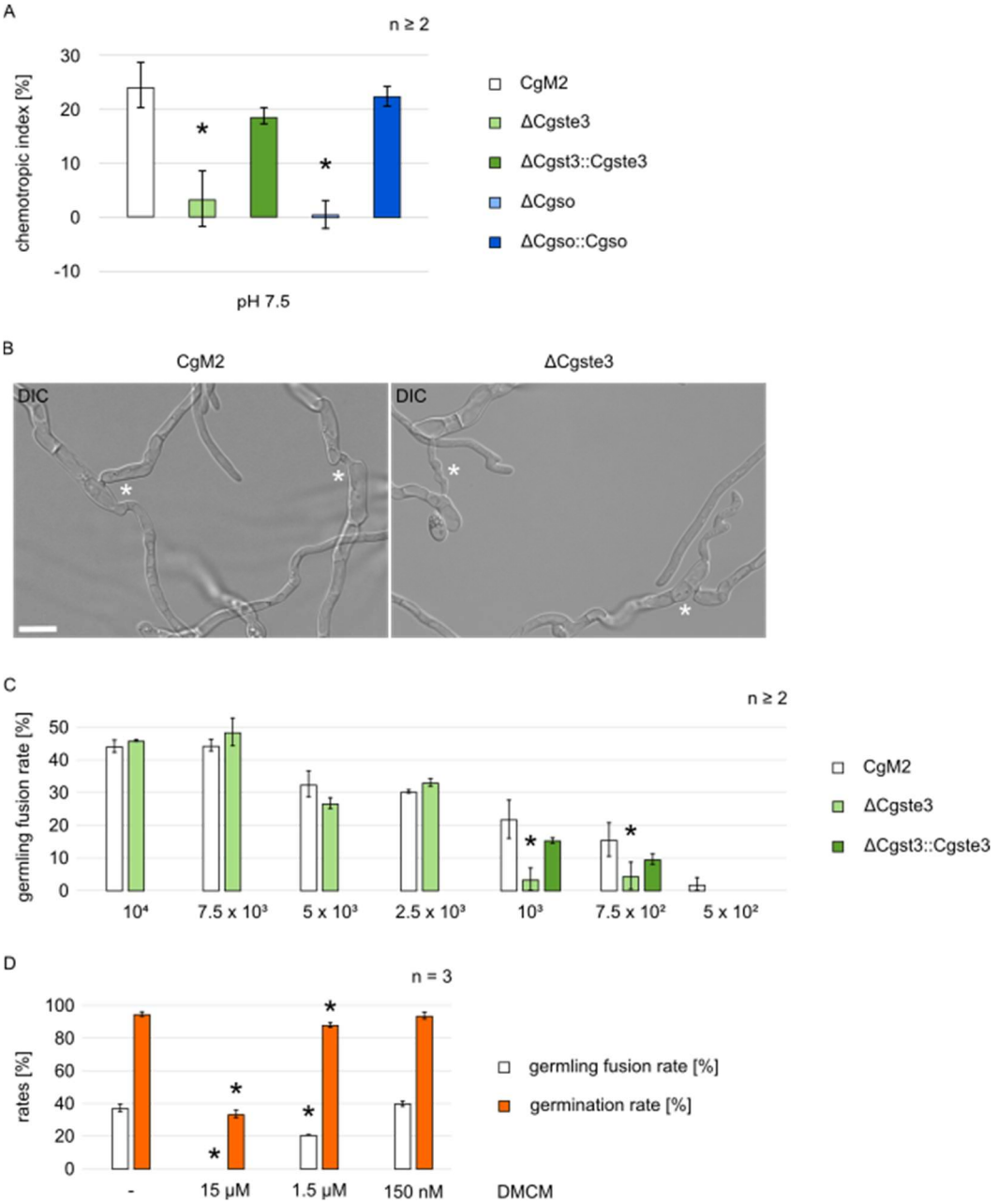

Figure 3 Sensing of acidic pH is mediated by the a-pheromone receptor CgSte3 and the CWI MAPK scaffold protein CgSo. (A) Chemotropic index of *C. graminicola* germlings of wildtype (CgM2), *Cgste3* and *Cgso* deletion strains and corresponding complementations to potassium phosphate buffer adjusted to pH 7.5. 20 µl of oval conidia (c = 5 x 10^5 ml^{-1}) were applied in a 3D printed device between two wells containing 40 µl solvent control and attractant. Microscopic evaluation of fungal tip growth was performed after incubation for 6 h, 23°C for least two biological replicates, statistical significance was calculated with a two-tailed t-test to CgM2 (*, $p < 0.05$). (B) Microscopic evaluation of germling fusions after spreading of 50 µl *C. graminicola* wildtype (CgM2) or Δ*Cgste3* oval conidia spore solutions (c = 5 x 10^7 ml^{-1}) on water agar (1% serva agar, 1% agarose, 25 mM $NaNO_3$) and incubation for 17 h, 23°C, scale = 10 µm, fusions are indicated with white asterisk. (C) Spore concentration-dependent germling fusion rates of *C. graminicola* wildtype, Δ*Cgste3* and Δ*Cgste3* complementation strain Δ*Cgste3*::*Cgste3*. 10 µl of oval conidia spore solutions were dropped on water agar (1% serva agar, 1% agarose, 25 mM $NaNO_3$) to reach spore amounts of 10^4 - 5 x 10^2. Microscopic evaluation after 17 h of incubation at 23°C was performed for at least 100 contacting germlings and conidia in higher spore concentration. In lower spore concentrations, the full area was examined for fusion bridge formation, n ≥ 2, statistical significance was calculated with a two-tailed t-test to CgM2 values of the corresponding spore concentration (*, $p < 0.05$). (D) Germling fusion and germination rates of *C. graminicola* wildtype in dependence of treatment with the PmaI inhibitor Demethoxycurcumin (DMCM). 20 µl of different DMCM

403 concentrations or the control were applied on dried 10 µl drops of oval conidia (c = 10^6 ml^{-1}) on water
404 agar (1% serva agar, 1% agarose, 25 mM $NaNO_3$) and dried prior to incubation for 17 h at 23°C. Since
405 DMCM was dissolved in DMSO, diluted DMSO equalizing 15 µM DMCM solutions were used as control.
406 Germling fusion was accessed for at least 100 contacting conidia or germlings. Germination rates were
407 determined by evaluating at least 100 conidian, n = 3, statistical significance was calculated with a two-
408 tailed t-test to control conditions (-), *, $p < 0.05$.

409

410 Together these results indicate, that indeed all three fungi share a common interaction signal,
411 but indicate also species-specific signals, explaining the higher proportion of self-interactions
412 observed. To test whether the shard interaction signal might be pH, conidia of all three species
413 were grown on Vogel's MM adjusted to different pH without buffering the medium. As seen for
414 *C. graminicola* on water agar, interaction frequency of all three species is pH dependent,
415 although to different extents: *C. graminicola* shows the most pH-stable interaction pattern,
416 reduced only significantly at basic pHs (Figure 4 E). The interaction frequency of *B. cinerea*
417 already dropped at pH 7, and in *N. crassa*, pH of 6.5 already reduced interaction rates
418 significantly. A similar pattern can be seen for the germination of conidia on Vogel's MM.
419 Germination rates of *C. graminicola* oval conidia is hardly affected also at high pH and the
420 germination rates of *B. cinerea* are stable until pH 9. However, *N. crassa* conidia are highly
421 sensitive to pH changes, showing already significant reduction on medium pH of 6.5
422 (Supplementary Figure 5).

423

424 Discussion

425 The perception of extracellular signals is important for fungi to find nutrients, hosts, toxic
426 environments, or germlings and spores of the same species (Turrà *et al.*, 2016). In this study,
427 we identified pH as a communication signal outgoing from secretomes harvested during
428 germling fusion. Already in earlier studies, pH was identified as a fusion-modulation factor:
429 over a broad pH range fusions *Fusarium oxysporum* take place, however, when the medium
430 is buffered, only pH of 6.4 still allows fusion to occur (Kurian et al., 2018). From those results,
431 it was concluded that an active modulation of pH by the fungal germlings are required for
432 germling fusion. In our experiments, we see a similar influence on pH of fusion frequency of
433 *C. graminicola*: whereas not-buffered media allow fusions over a broad pH spectrum, buffering
434 abolishes fusion bridge formation. Analysis of chemotropic growth further emphasized the role
435 of distinct pHs (7.5) on germling attraction and thus their signaling nature (Figure 2). Likewise,
436 acidic pH was shown to induce chemotropic growth in germlings of *Aspergillus nidulans*
437 (Yamamoto *et al.*, 2024). We further identified the plasma membrane localized ATPase PmaI
438 as probable source for pH gradient formation using the specific PmaI-inhibitor
439 Demthoxycurcumin (Dao et al., 2016). In fungi and plants, PmaI ATPase-formed pH gradient
440 drive the uptake of nutrients and its activity is directly linked to cell growth (Serrano, 1984,
441 Divon and Fluhr, 2007, Yamamoto et al., 2024, Palmgren, 2001, Haruta *et al.*, 2010,
442 Morsomme and Boutry, 2000). Additionally to the provision of an extracellular proton gradient,
443 PmaI activity results in a lower cytosolic pH, which is involved in the regulation of MAPK
444 pathways and thus affects development and pathogenicity in *F. oxysporum* (Mariscal *et al.*,
445 2022). Intriguingly, PmaI was also shown to be crucial for the sensing of acidic pH in *A.*
446 *nidulans*, however it is unclear how the determining mechanism works (Yamamoto et al.,
447 2024).

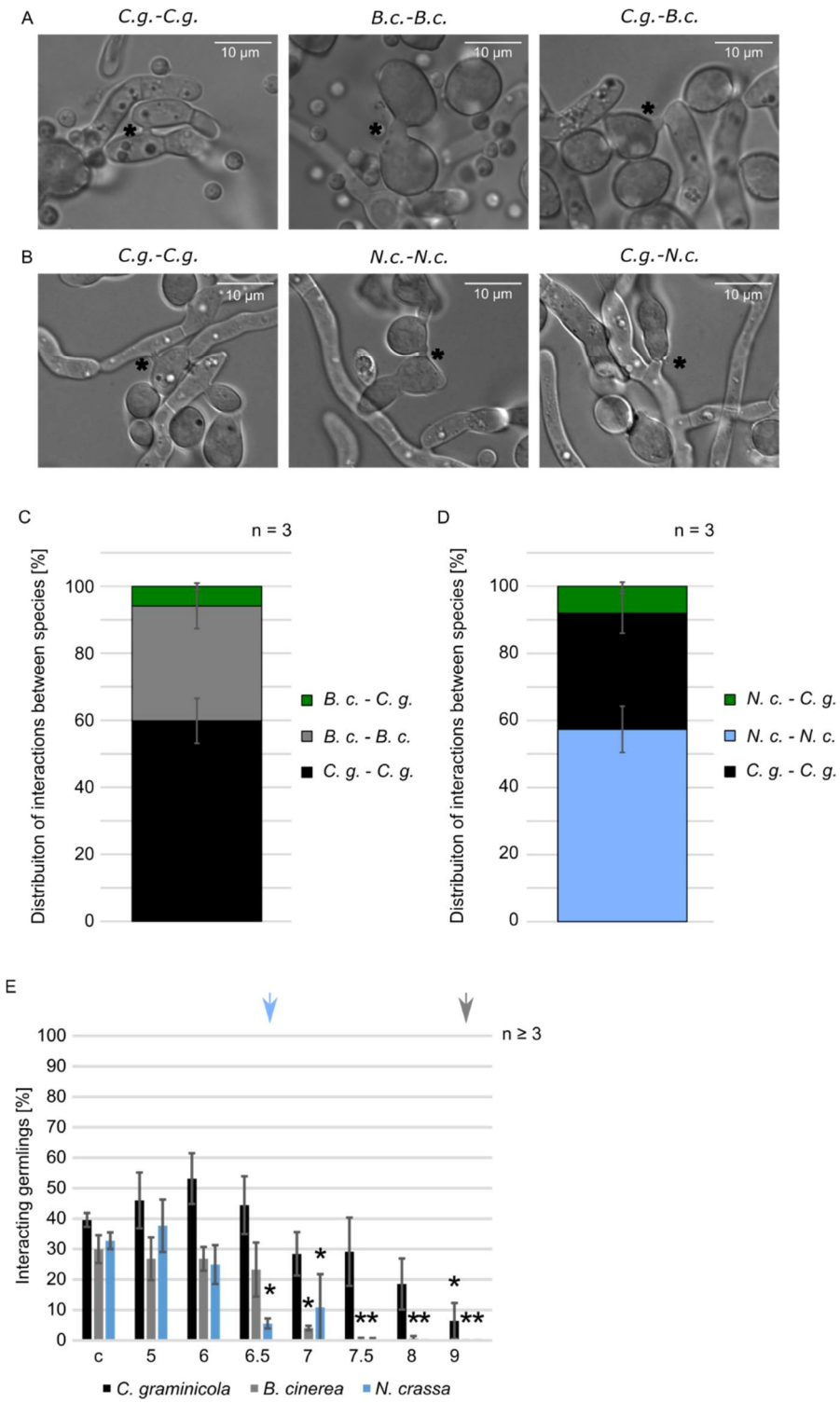

Figure 4 Interaction of *C. graminicola* with *N. crassa* and *B. cinerea*. (A-D) Inter- and Intraspecies interactions of *C. graminicola* and *B. cinerea* or *N. crassa* on Vogels minimal medium (MM). (A, C) The interactions experiment with *C. graminicola* and *B. cinerea* was carried out at 23°C with an incubation time of 17 h. First, *C. graminiocla* oval conidia (50 µl of c = 5 x 10^7 ml^{-1}) and 300 µl *B. cinerea* spore solution (c= 3.33 x 10^7 ml^{-1}) were spread together on Vogels' MM. (B, D) To access *C. graminicola* and *N. crassa* germling interactions, 50 µl of a *C. graminicola* oval conidia spore solution (c = 5x10^7 x ml^{-1}) was distributed on incubation medium and incubated for 14 h at 23°C. After that time, 300µl of *N. crassa* spore solution (c = 10^7 ml^{-1}) was added on those pre-incubated plates and further incubated at 28°C for 3.5 - 4 h. (A-B) Microscopic images of intra- and interspecies interaction, interactions are marked with a black asterisk, scale = 10 µm. (C-D) Inter- and intraspecies interaction rates of ≥ 76 germling interactions of *C. graminicola* and *B. cinerea* (C) and *C. graminicola* with *N. crassa* (D), n = 3. (E) Germling interaction

460 rates of *C. graminicola*, *B. cinerea* and *N. crassa* on Vogel's minimal medium adjusted to different pH.
461 Species-specific conidia amounts (*C. graminicola*: 50 µl of 5 x 10^7 ml^{-1}; *B. cinerea* and *N. crassa*: 300
462 µl of c = 10^7 ml^{-1}) were spread on Vogels' MM and incubated at 23°C for 17 h (*C. graminicola*, *B. cinerea*)
463 or 28°C for 3,5 - 4 h (*N. crassa*), n ≥ 3, statistical significance was calculated with a two-tailed t-test to
464 control conditions (c), *, $p < 0.05$.

465

466 pH is a crucial environmental factor for fungi and its fluctuations influence diverse cellular
467 processes like cell wall remodeling, nutrient availability, and enzyme activity (Li *et al.*, 2021).
468 Many plant and human pathogenic fungi modulate the extracellular pH to explore their
469 surroundings, enable successful host infection and maintain cellular homeostasis (Masachis
470 *et al.*, 2016, Fernandes *et al.*, 2017, Kane, 2016, Alkan *et al.*, 2013, Vylkova, 2017, Kesten *et*
471 *al.*, 2019). Traditionally, plant-interacting fungi were thought to be strictly alkalizing or acidifying
472 their surroundings. However, in the last decade it was shown, that induced changes in ambient
473 pH are flexible and depend on carbon availability (Bi *et al.*, 2016). Sensing of extracellular,
474 alkaline pH is primarily mediated by the pal/RIM pathway in fungi, with PalH as the central pH
475 sensor (Selvig and Alspaugh, 2011). Together with MAPK modules, the pal/RIM pathway is
476 central for the sensing and the response to extracellular pH levels, enabling to maintain cellular
477 integrity also in the face of stress and pathogenic host interaction (Lara-Martínez *et al.*, 2025).
478 PalH is a 7 transmembrane receptor resembling classical G-protein coupled receptors
479 (GPCR), interacting downstream with an arrestin for signal transduction (Lucena-Agell *et al.*,
480 2016). As transcription factor downstream of PalH, PacC is described, acting as activator of
481 gene expression at alkaline pH and as a repressor of genes expressed at acidic pH (Lara-
482 Martínez et al., 2025). In contrast, the sensor for acidic environmental pH is unknown in fungi
483 (Yamamoto et al., 2024). In this study, we provide evidence that the a-pheromone receptor
484 CgSte3 mediates sensing of acidic pH gradients, activating downstream the CWI pathway
485 (Figure 3). Fungal pheromone receptors are GPCRs first described in the yeast
486 *Saccharomyces cerevisiae*, in which they mediate chemotropic attraction of mating partners
487 during sexual fusion (Hagen and Sprague Jr, 1984, Nakayama *et al.*, 1985, Jenness *et al.*,
488 1986). In the last years, new roles for fungal pheromone receptors were identified. This
489 includes the spore density dependent regulation of germination in *F. oxysporum*, and the
490 sensing of plant defense molecules like class III peroxidases and diterpenoids in different host-
491 pathogen systems (Turrà et al., 2015, Vitale et al., 2019, Sharma et al., 2022, Rudolph et al.,
492 2024a, Rudolph et al., 2024b). Downstream of diterpenoid and peroxidase sensing, in those
493 studies the CWI was shown to be responsible for consequent growth redirection (Turrà et al.,
494 2015, Sharma et al., 2022, Rudolph et al., 2024b), indicating a conserved link between external
495 signal sensing by pheromone receptors and CWI activation. So far, only one study investigated
496 how the two pheromone receptors interact upon peroxidase sensing. These results point to a
497 scenario, in which peroxidase directly or a peroxidase-generated ligand stimulates heterodimer
498 formation in between Ste2 and Ste3 of *Fusarium graminearum* (Sharma et al., 2022).
499 Intriguingly, *C. graminicola* is the only species, in which the α-pheromone receptor Ste2 was
500 lost during evolution (Wilson *et al.*, 2021) and therefore the recognition of external signals is
501 dependent only on the a-pheromone receptor Ste3. How the perception in this one-receptor
502 system functions on the molecular level, is still to be explored. Another open question is how
503 those different attractant molecules are sensed by the same receptor. Since the chemical
504 properties of the perceived signals are such diverse, a direct ligand-receptor interaction seems
505 unlikely. For mammalian cells it was shown that GPCRs and growth factor receptor tyrosine
506 kinases (RTKs) can activate each other in a process termed 'transactivation', without the
507 requirement for ligand binding to the secondary receptor (Wang, 2016, Delcourt *et al.*, 2007).
508 In such a scenario, the a-pheromone receptor CgSte3 could be associated with other, more
509 specific receptors, which serve as sensors for diterpenoids, peroxidases or pH specifically.
510 Additionally, modifications of amino acids can induce GPCR activation (Wang *et al.*, 2018). In

511 mammalian cells, a current study shows that protonation of histidine residues can induce
512 GPCR activation (Guo *et al.*, 2025). As a third possibility, pH could influence the binding-
513 capacity of another ligand by CgSte3, resulting in receptor activation (Sun *et al.*, 2025). Which
514 of these possibilities or also other probable mechanisms are mediating CgSte3 receptor
515 activation, has to be investigated in future studies.

516 Together, our results about *C. graminicola* CAT fusion point to a scenario, in which PmaI-
517 depenent pH gradients are formed as soon as a conidium starts to germinate. Those pH
518 gradients are sensed by surrounding germlings or conidia via the a-pheromone receptor
519 CgSte3, resulting in the activation of CWI and induction of growth redirection towards the
520 interaction partner. From work in other fungi, especially *N. crassa*, we know the oscillatory
521 recruitment of SO and MAK-2 during germling interaction is crucial for fusion bridge formation
522 (Fleissner et al., 2009, Serrano et al., 2018). Since CgSo is a scaffold of CWI, pH sensing
523 might additionally induce CgSo localization to the plasma membrane, which could be
524 associated with the secretion of a second interaction signal, still to be discovered (Figure 5).
525 This model could also explain why germling fusions are absent in falcate conidia: those spores
526 have a pronounced dormant phase, mediated by secondary metabolites like mycosporines
527 and other factors (Leite and Nicholson, 1992, Vasselli *et al.*, 2022, Chaky et al., 2001). Since
528 germination of falcate conidia does not occur under starvation conditions, PmaI is inactive and
529 no pH gradients build up, making an induction of the fusion process impossible. However,
530 when oval conidia are close by, they can provide the pH fusion-initiation signal, which is
531 perceived by falcate conidia and subsequently induce dormancy breaking, germling
532 interaction, and fusion.

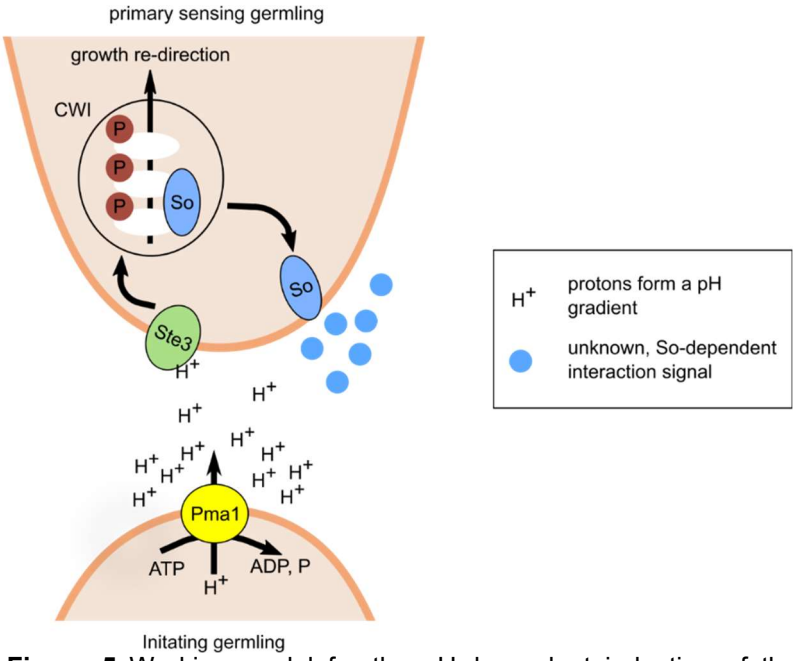

533 **Figure 5** Working model for the pH-dependent induction of the cell dialogue. PmaI-depenent pH
534 gradients (H^+) form immediately when a conidium starts to germinate. Those pH gradients are sensed
535 by surrounding germlings or conidia via the a-pheromone receptor Ste3, resulting in the activation of the
536 Cell Wall Integrity (CWI) MAPK pathway and induction of growth redirection towards the interaction
537 partner. From work in other fungi, we propose that CWI activation by Ste3 induces the relocalization of
538 SO to the tip of the interacting germling, followed by the release of a SO-dependent, so far unknown
539 communication signal (blue circles).

540

541 The ability of germlings to fuse in an early stage of colony formation, fastens radial growth, by
542 sharing of nutrients or cellular components (Roca *et al.*, 2005, Richard et al., 2012). Recently,
543 studies have shown that germling communication mediating bidirectional chemotropic growth

544 prior to fusion is not species-specific (Haj Hammadeh et al., 2022). Closely related species of
545 *Colletotrichum* and *Aspergillus* are even able to fuse and exchange genetic material, resulting
546 in progeny with recombinant genomes (Ishitani *et al.*, 1956, Mehta and Baghela, 2021). In this
547 study, we show that the maize pathogen *C. graminicola* communicates with the saprophyte
548 *N. crassa* and the pathogen *B. cinerea* with 8 and 6 % of interactions respectively. The three
549 species differ strongly in their preferred habitat. *N. crassa* is a saprophytic fungus primarily
550 living on burned vegetation in humid subtropical and tropical regions (Turner *et al.*, 2001).
551 *B. cinerea*, the grey mold-causing fungus, has a high host range including several vegetables
552 like tomato, lettuce, and beans, or fruit crops such as strawberries and grapes (Chen *et al.*,
553 2023). Even though *B. cinerea* cause lesions on *Zea mays* under artificial conditions, cereals
554 are not host plants of the pathogen (Bi *et al.*, 2023), thus it is unlikely that those fungi meet in
555 the environment. In line, we never observed the outgrowth of new fungal hyphae from the
556 contact point of intraspecies interactions, as it was reported for the interaction of *C. siamense*
557 and *C. gloeosporioides* (Mehta and Baghela, 2021). Intriguingly, the two pathogenic species
558 *B. cinerea* and *C. graminicola* showed more stable fusion and germination frequencies as the
559 saprophytic fungus *N. crassa*. This is in line with previous observations that especially plant-
560 interacting species are able to tolerate wide ranges of ambient pH (Felix *et al.*, 1993).

561 In conclusion, our study has provided new insights into the molecular mechanisms underlying
562 germling fusion in the maize pathogen *C. graminicola*. We have identified pH as a
563 communication signal outgoing from secretomes harvested during the germling fusion, and
564 have shown that the plasma membrane localized ATPase PmaI is a probable source for pH
565 gradient formation. Our results also suggest that the a-pheromone receptor CgSte3 mediates
566 sensing of acidic pH gradients, activating downstream the CWI MAPK pathway. These findings
567 are consistent with previous studies that have shown that pH is a crucial environmental factor
568 for fungi and its fluctuations influence diverse cellular processes. Our results also suggest that
569 the maize pathogen *C. graminicola* communicates with the saprophyte *N. crassa* and the grey
570 mold *B. cinerea*, although these three species differ strongly in their preferred habitat. Overall,
571 our study contributes to a better understanding of the molecular mechanisms underlying
572 germling fusion in fungi and indicate pH as fusion initiation signal across species borders.

573

574 <u>Acknowledgments</u>

575 We thank Gabriele Beyer and Gertrud Stahlhut for excellent technical assistance and Lilith
576 Elisabeth Gück and Simone Lewandowski for help with experimental work. This work was
577 funded by the Deutsche Forschungsgemeinschaft (Bonn-Bad Godesberg). Grant was provided
578 to D.E.N. (project NO 1230/3-1 (447175909). This work was partly supported by the Göttingen
579 Graduate Center for Neurosciences, Biophysics, and Molecular Biosciences at the Georg-
580 August-Universität Göttingen.

581

582 <u>References</u>

583 Alkan, N., Espeso, E. A. and Prusky, D. (2013) "Virulence regulation of phytopathogenic fungi
584 by pH." *Antioxidants & Redox Signaling,* 19**,** 1012-1025.
585 Bastiaans, E., Debets, A. J. and Aanen, D. K. (2015) "Experimental demonstration of the
586 benefits of somatic fusion and the consequences for allorecognition." *Evolution,* 69**,**
587 1091-1099.
588 Belisário, R., Robertson, A. E. and Vaillancourt, L. J. (2022) "Maize anthracnose stalk rot in
589 the genomic era." *Plant Disease,* 106**,** 2281-2298.

590 Bi, F., Barad, S., Ment, D., et al. (2016) "Carbon regulation of environmental pH by secreted
591 small molecules that modulate pathogenicity in phytopathogenic fungi." *Molecular plant*
592 *pathology,* 17**,** 1178-1195.
593 Bi, K., Liang, Y., Mengiste, T. and Sharon, A. (2023) "Killing softly: a roadmap of *Botrytis*
594 *cinerea* pathogenicity." *Trends in plant science,* 28**,** 211-222.
595 Chaky, J., Anderson, K., Moss, M. and Vaillancourt, L. (2001) "Surface hydrophobicity and
596 surface rigidity induce spore germination in *Colletotrichum graminicola*."
597 *Phytopathology,* 91**,** 558-564.
598 Chen, T., Zhang, Z., Chen, Y., Li, B. and Tian, S. (2023) "*Botrytis cinerea*." *Current Biology,*
599 33**,** R460-R462.
600 Dao, T. T., Sehgal, P., Tung, T. T., et al. (2016) "Demethoxycurcumin is a potent inhibitor of
601 p-type ATPases from diverse kingdoms of life." *PLoS One,* 11**,** e0163260.
602 Delcourt, N., Bockaert, J. and Marin, P. (2007) "GPCR-jacking: from a new route in RTK
603 signalling to a new concept in GPCR activation." *Trends in pharmacological sciences,*
604 28**,** 602-607.
605 Divon, H. H. and Fluhr, R. (2007) "Nutrition acquisition strategies during fungal infection of
606 plants." *FEMS microbiology letters,* 266**,** 65-74.
607 Felix, G., Regenass, M. and Boller, T. (1993) "Specific perception of subnanomolar
608 concentrations of chitin fragments by tomato cells: induction of extracellular
609 alkalinization, changes in protein phosphorylation, and establishment of a refractory
610 state." *The Plant Journal,* 4**,** 307-316.
611 Fernandes, T. R., Segorbe, D., Prusky, D. and Di Pietro, A. (2017) "How alkalinization drives
612 fungal pathogenicity." *PLoS pathogens,* 13**,** e1006621.
613 Fischer, M. S. and Glass, N. L. (2019) "Communicate and fuse: how filamentous fungi establish
614 and maintain an interconnected mycelial network." *Frontiers in microbiology,* 10**,** 619.
615 Fleissner, A., Leeder, A. C., Roca, M. G., Read, N. D. and Glass, N. L. (2009) "Oscillatory
616 recruitment of signaling proteins to cell tips promotes coordinated behavior during cell
617 fusion." *Proceedings of the National Academy of Sciences,* 106**,** 19387-19392.
618 Forgey, W., Blanco, M. and Loegering, W. (1978) "Differences in pathological capabilities and
619 host specificity of *Colletotrichum graminicola* on *Zea mays*." *Plant Disease Reporter,*
620 62**,** 573-576.
621 Fu, C., Iyer, P., Herkal, A., Abdullah, J., Stout, A. and Free, S. J. (2011) "Identification and
622 characterization of genes required for cell-to-cell fusion in *Neurospora crassa*."
623 *Eukaryotic cell,* 10**,** 1100-1109.
624 Glass, N. L., Rasmussen, C., Roca, M. G. and Read, N. D. (2004) "Hyphal homing, fusion and
625 mycelial interconnectedness." *Trends in microbiology,* 12**,** 135-141.
626 Guo, L., Zhu, K., Zhong, Y.-N., et al. (2025) "Structural basis and biased signaling of proton
627 sensation by GPCRs mediated by extracellular histidine rearrangement." *Molecular*
628 *Cell,* 85**,** 1658-1673. e1657.
629 Hagen, D. C. and Sprague Jr, G. F. (1984) "Induction of the yeast α-specific STE3 gene by the
630 peptide pheromone a-factor." *Journal of molecular biology,* 178**,** 835-852.
631 Haj Hammadeh, H., Serrano, A., Wernet, V., et al. (2022) "A dialogue-like cell communication
632 mechanism is conserved in filamentous ascomycete fungi and mediates interspecies
633 interactions." *Proceedings of the National Academy of Sciences,* 119**,** e2112518119.
634 Harris, S. L., Na, S., Zhu, X., et al. (1994) "Dominant lethal mutations in the plasma membrane
635 H (+)-ATPase gene of *Saccharomyces cerevisiae*." *Proceedings of the National*
636 *Academy of Sciences,* 91**,** 10531-10535.
637 Haruta, M., Burch, H. L., Nelson, R. B., et al. (2010) "Molecular characterization of mutant
638 *Arabidopsis* plants with reduced plasma membrane proton pump activity." *Journal of*
639 *Biological Chemistry,* 285**,** 17918-17929.
640 Heller, J., Zhao, J., Rosenfield, G., Kowbel, D. J., Gladieux, P. and Glass, N. L. (2016)
641 "Characterization of greenbeard genes involved in long-distance kind discrimination in
642 a microbial eukaryote." *PLoS biology,* 14**,** e1002431.
643 Herzog, S., Schumann, M. R. and Fleißner, A. (2015) "Cell fusion in *Neurospora crassa*."
644 *Current opinion in microbiology,* 28**,** 53-59.

Ishitani, C., Ikeda, Y. and Sakaguchi, K.-I. (1956) "Hereditary variation and genetic recombination in koji-molds (*Aspergillus oryzae* and *Asp. sojae*) VI. Genetic recombination in heterozygous diploids." *The Journal of General and Applied Microbiology,* 2**,** 401-430.

Jenness, D. D., Burkholder, A. C. and Hartwell, L. H. (1986) "Binding of α-factor pheromone to *Saccharomyces cerevisiae* a cells: dissociation constant and number of binding sites." *Molecular and cellular biology,* 6**,** 318-320.

Kane, P. M. (2016) Proton transport and pH control in fungi. In: *Yeast Membrane Transport.* Ramos, J., Sychrová, H. and Kschischo, M., eds.: Springer, pp. 33-68.

Kesten, C., Gámez-Arjona, F. M., Menna, A., et al. (2019) "Pathogen-induced pH changes regulate the growth-defense balance in plants." *The EMBO Journal,* 38**,** e101822.

Kurian, S. M., Di Pietro, A. and Read, N. D. (2018) "Live-cell imaging of conidial anastomosis tube fusion during colony initiation in *Fusarium oxysporum*." *PLoS One,* 13**,** e0195634.

Lara-Martínez, D., Tristán-Flores, F. E., Cervantes-Montelongo, J. A. and Silva-Martínez, G. A. (2025) "Fungal stress responses and the importance of GPCRs." *Journal of Fungi,* 11**,** 213.

Leite, B. and Nicholson, R. L. (1992) "Mycosporine-alanine: A self-inhibitor of germination from the conidial mucilage of *Colletotrichum graminicola*." *Experimental mycology,* 16**,** 76-86.

Li, B., Chen, Y. and Tian, S. (2021) "Function of pH-dependent transcription factor PacC in regulating development, pathogenicity, and mycotoxin biosynthesis of phytopathogenic fungi." *The FEBS Journal,* 289**,** 1723-1730.

Li, J., Yang, S., Li, D., Peng, L., Fan, G. and Pan, S. (2022) "The plasma membrane H^+-ATPase is critical for cell growth and pathogenicity in *Penicillium digitatum*." *Applied Microbiology and Biotechnology,* 106**,** 5123-5136.

Lucena-Agell, D., Hervás-Aguilar, A., Múnera-Huertas, T., et al. (2016) "Mutational analysis of the *Aspergillus* ambient pH receptor PalH underscores its potential as a target for antifungal compounds." *Molecular Microbiology,* 101**,** 982-1002.

Mariscal, M., Miguel-Rojas, C., Hera, C., Fernandes, T. R. and Di Pietro, A. (2022) "*Fusarium oxysporum* casein kinase 1, a negative regulator of the plasma membrane H^+-ATPase Pma1, is required for development and pathogenicity." *Journal of Fungi,* 8**,** 1300.

Masachis, S., Segorbe, D., Turrà, D., et al. (2016) "A fungal pathogen secretes plant alkalinizing peptides to increase infection." *Nature Microbiology,* 1**,** 1-9.

Mehta, N. and Baghela, A. (2021) "Quorum sensing-mediated inter-specific conidial anastomosis tube fusion between *Colletotrichum gloeosporioides* and *C. siamense*." *IMA fungus,* 12**,** 1-17.

Morsomme, P. and Boutry, M. (2000) "The plant plasma membrane H^+-ATPase: structure, function and regulation." *Biochimica et Biophysica Acta (BBA)-Biomembranes,* 1465**,** 1-16.

Nakayama, N., Miyajima, A. and Arai, K. (1985) "Nucleotide sequences of STE2 and STE3, cell type-specific sterile genes from *Saccharomyces cerevisiae*." *The EMBO journal,* 4**,** 2643.

Nordzieke, D. E. (2022) "Hyphal fusions enable efficient nutrient distribution in *Colletotrichum graminicola* conidiation and symptom development on maize." *Microorganisms,* 10**,** 1146.

Nordzieke, D. E., Sanken, A., Antelo, L., Raschke, A., Deising, H. B. and Pöggeler, S. (2019) "Specialized infection strategies of falcate and oval conidia of *Colletotrichum graminicola*." *Fungal Genetics and Biology,* 133**,** 103276.

O'Connell, R. J., Thon, M. R., Hacquard, S., et al. (2012) "Lifestyle transitions in plant pathogenic *Colletotrichum* fungi deciphered by genome and transcriptome analyses." *Nature genetics,* 44**,** 1060-1065.

Palmgren, M. G. (2001) "Plant plasma membrane H^+-ATPases: powerhouses for nutrient uptake." *Annual review of plant biology,* 52**,** 817-845.

Panaccione, D. G., Vaillancourt, L. J. and Hanau, R. M. (1989) "Conidial dimorphism in *Colletotrichum graminicola*." *Mycologia,* 81**,** 876-883.

Portillo, F. (2000) "Regulation of plasma membrane H^+-ATPase in fungi and plants." *Biochimica et Biophysica Acta (BBA)-Reviews on Biomembranes,* 1469**,** 31-42.

Quidde, T., Büttner, P. and Tudzynski, P. (1999) "Evidence for three different specific saponin-detoxifying activities in *Botrytis cinerea* and cloning and functional analysis of a gene coding for a putative avenacinase." *European Journal of Plant Pathology,* 105**,** 273-283.

Ramaswe, J. B., Steenkamp, E. T., De Vos, L., Fru, F. F., Adegeye, O. O. and Wingfield, B. D. (2024) "Sex pheromone receptor Ste2 orchestrates chemotropic growth towards pine root extracts in the pitch canker pathogen *Fusarium circinatum*." *Pathogens,* 13**,** 425.

Read, N. D., Goryachev, A. B. and Lichius, A. (2012) "The mechanistic basis of self-fusion between conidial anastomosis tubes during fungal colony initiation." *Fungal Biology Reviews,* 26**,** 1-11.

Richard, F., Glass, N. and Pringle, A. (2012) "Cooperation among germinating spores facilitates the growth of the fungus, *Neurospora crassa*." *Biology Letters,* 8**,** 419-422.

Roca, G. M., Read, N. D. and Wheals, A. E. (2005) "Conidial anastomosis tubes in filamentous fungi." *FEMS microbiology letters,* 249**,** 191-198.

Rudolph, A., Schunke, C., Sasse, C., et al. (2024a) "Maize diterpenoid sensing via Ste3 a-pheromone receptor and rapid germination of *Colletotrichum graminicola* oval conidia facilitating root infection." *bioRxiv***,** 2024.2004. 2005.588234.

Rudolph, A. Y., Schunke, C. and Nordzieke, D. E. (2024b) "Conserved perception of host and non-host signals via the a-pheromone receptor Ste3 in *Colletotrichum graminicola*." *Frontiers in Fungal Biology,* 5**,** 1454633.

Ruxton, G. D. (2006) "The unequal variance t-test is an underused alternative to Student's t-test and the Mann–Whitney U test." *Behavioral Ecology,* 17**,** 688-690.

Schunke, C., Pöggeler, S. and Nordzieke, D. E. (2020) "A 3D printed device for easy and reliable quantification of fungal chemotropic growth." *Frontiers in Microbiology,* 11**,** 584525.

Selvig, K. and Alspaugh, J. A. (2011) "pH response pathways in fungi: adapting to host-derived and environmental signals." *Mycobiology,* 39**,** 249-256.

Serrano, A., Illgen, J., Brandt, U., et al. (2018) "Spatio-temporal MAPK dynamics mediate cell behavior coordination during fungal somatic cell fusion." *Journal of cell science,* 131**,** jcs213462.

Serrano, R. (1984) "Plasma membrane ATPase of fungi and plants as a novel type of proton pump." *Current topics in cellular regulation,* 23**,** 87-126.

Sharma, T., Sridhar, P. S., Blackman, C., et al. (2022) "*Fusarium graminearum* Ste3 G-protein coupled receptor: A mediator of hyphal chemotropism and pathogenesis." *Msphere,* 7**,** e00456-00422.

Sridhar, P. S., Trofimova, D., Subramaniam, R., et al. (2020) "Ste2 receptor-mediated chemotropism of *Fusarium graminearum* contributes to its pathogenicity against wheat." *Scientific Reports,* 10**,** 10770.

Sun, L., Su, T., Fisher, A. C., et al. (2025) "Dynamic protonation of ligand sites in molecular catalysts enhances electrochemical CO_2 reduction." *Science Advances,* 11**,** eadu6915.

Turner, B. C., Perkins, D. D. and Fairfield, A. (2001) "*Neurospora* from natural populations: a global study." *Fungal Genetics and Biology,* 32**,** 67-92.

Turrà, D., El Ghalid, M., Rossi, F. and Di Pietro, A. (2015) "Fungal pathogen uses sex pheromone receptor for chemotropic sensing of host plant signals." *Nature,* 527**,** 521-524.

Turrà, D., Nordzieke, D., Vitale, S., El Ghalid, M. and Di Pietro, A. (2016) Hyphal chemotropism in fungal pathogenicity. In: *Seminars in cell & developmental biology.* Elsevier, pp. 69-75.

Vasselli, J. G., Hancock, H., Bedsole, C. O., Kainer, E., Chappell, T. M. and Shaw, B. D. (2022) "The conidial coin toss: A polarized conidial adhesive in *Colletotrichum graminicola*." *Fungal Genetics and Biology,* 163**,** 103747.

754 Vitale, S., Di Pietro, A. and Turrà, D. (2019) "Autocrine pheromone signalling regulates
755 community behaviour in the fungal pathogen *Fusarium oxysporum*." *Nature*
756 *microbiology,* 4**,** 1443-1449.
757 Vogel, H. J. (1956) "A convenient growth medium for *Neurospora* (Medium N)." *Microbial*
758 *Genet. Bull.,* 13**,** 42-43.
759 Vylkova, S. (2017) "Environmental pH modulation by pathogenic fungi as a strategy to conquer
760 the host." *PLoS pathogens,* 13**,** e1006149.
761 Wang, W., Qiao, Y. and Li, Z. (2018) "New insights into modes of GPCR activation." *Trends in*
762 *pharmacological sciences,* 39**,** 367-386.
763 Wang, Z. (2016) "Transactivation of epidermal growth factor receptor by G protein-coupled
764 receptors: recent progress, challenges and future research." *International journal of*
765 *molecular sciences,* 17**,** 95.
766 Wilson, A. M., Lelwala, R. V., Taylor, P. W., Wingfield, M. J. and Wingfield, B. D. (2021)
767 "Unique patterns of mating pheromone presence and absence could result in the
768 ambiguous sexual behaviors of *Colletotrichum* species." *G3,* 11**,** jkab187.
769 Yamamoto, R., Miki, H., Itani, A. and Takeshita, N. (2024) "Hyphae of the fungus *Aspergillus*
770 *nidulans* demonstrate chemotropism to nutrients and pH." *Plos Biology,* 22**,** e3002726.
771 Zhgun, A., Dumina, M., Valiakhmetov, A. and Eldarov, M. (2020) "The critical role of plasma
772 membrane H^+-ATPase activity in cephalosporin C biosynthesis of *Acremonium*
773 *chrysogenum*." *PLoS One,* 15**,** e0238452.